Research Article

Preparation of hcp and fcc Ni and Ni/NiO Nanoparticles Using a Citric Acid Assisted Pechini-Type Method

L. A. García-Cerda,[1] K. M. Bernal-Ramos,[2] Sagrario M. Montemayor,[2] M. A. Quevedo-López,[3] R. Betancourt-Galindo,[1] and D. Bueno-Báques[1]

[1] *Departamento de Materiales Avanzados, Centro de Investigación en Química Aplicada, Boulevard. Enrique Reyna Hermosillo #140, CP 25253 Saltillo, COAH, Mexico*

[2] *Facultad de Ciencias Químicas, Universidad Autónoma de Coahuila, Boulevard. V. Carranza e Ing. José Cárdenas V. s/n, 25280 Saltillo, COAH, Mexico*

[3] *Department of Materials Science and Engineering, University of Texas at Dallas, Richardson, TX 75080, USA*

Correspondence should be addressed to L. A. García-Cerda, lagarcia@ciqa.mx

The preparation and characterization of hcp and fcc Ni and Ni/NiO nanoparticles is reported. Ni and Ni/NiO nanoparticles were obtained starting from a precursor material prepared using a citric assisted Pechini-type method and, then, followed by a calcination of the precursor in air at either 400 or 600°C for different times. The precursor was analyzed using thermogravimetric and differential thermal methods (TGA-DTA), and the resulting nanoparticles were characterized by X-ray diffraction (XRD), high-resolution transmission electron microscopy (HRTEM), and vibrational sample magnetometry. Nanoparticles showed a phase transformation for Ni from hcp to fcc and/or to fcc NiO structure as the calcination time increased. The influence of the phase transition and the formation of NiO on the magnetic properties of the samples are discussed.

1. Introduction

The study of different types of nanoparticles has been an extremely active research area in the last decade. Nanoparticles are very promising for new applications due to the fact that a similar chemical composition can lead to different properties compared to bulk, microcrystalline powders, or thin films. In particular, the synthesis of Ni and Ni/NiO nanoparticles has received considerable attention, based on their interesting properties for applications in ferrofluids, catalysis, magnetic materials, gas sensors, and biomedical applications [1–5].

To the date, different methods have been used to prepare Ni and Ni/NiO nanoparticles, which include thermal reduction process [6], ball milling [3], organometallic route [7], and magnetron plasma [8]. The Pechini method [9] is a solution-based technique that has several advantages over other methods (either mechanical or chemical). This process

allows obtaining materials with excellent homogeneity, composition control, and lower processing temperatures. This method is also simple, cost effective, and versatile with the additional advantage of its low temperature requirements. The general idea of this method is to homogeneously distribute the metallic cations in a polymeric resin precursor, while inhibiting its segregation and precipitation from the solution. A further calcination of this precursor at a relatively low temperatures results in homogeneous nanoparticles.

In the present work, we report the synthesis of hcp and fcc Ni and Ni/NiO nanoparticles using a citric acid assisted Pechini-type method. We show that this method allows precise control of the structure of the nanoparticles through some easily adjustable processing parameters. Also herein we assess the influence of the processing conditions on the structural, morphological, and magnetic properties of nanoparticles through the analysis of X-ray diffraction (XRD), high-resolution transmission electron microscopy (TEM), and VSM measurements results.

2. Experimental

The chemicals used in this study were analytical grade purity: nickel chloride (NiCl$_2$·6H$_2$O, Aldrich Co.), citric acid (C$_6$H$_8$O$_7$·H$_2$O, Aldrich Co.) and ethylene glycol (C$_2$H$_6$O$_2$, Aldrich Co.), and distilled water. All reagents were used as received. The precursor material was prepared as follows: first, citric acid was dissolved in distilled water, and then nickel chloride was added to the citric acid solution and stirred until a clear and homogeneous solution was obtained. Finally, ethylene glycol was added, and the resulting solution was stirred and then heated at 100°C to slowly evaporate the solution until a highly viscous resin was generated. The resin was then dried at 130°C, milled, and calcinated in air at 400 or 600°C for 15 min, 1 h, and 2 h, depending on the sample.

The thermal decomposition of the precursor material was evaluated by simultaneous TGA/DTA analysis (Shimadzu TGA-50/DTA-50 thermoanalyzer). The phase identification of the obtained nanoparticles was recorded by X-ray diffractometer (Siemens D5000) with CuKα radiation at 35 kV and 25 mA at a scan rate of 0.02 (2θ)/s. The phase percentages of the samples were determined by whole-profile fitting (WPF) using Jade 6 software developed by Material Data, Inc. The size and morphology of the nanoparticles were observed directly using a high-resolution transmission electron microscopic (HRTEM) (FEI TITAN HRTEM). Hysteresis loops of the resultant nanoparticles were recorded at room temperature using a VSM (Quantum Design, PPMS 6000).

3. Results and Discussion

The TGA and DTA curves of the precursor material are shown in Figure 1. The weight loss of the precursor material is complete at ~550°C. Three discrete weight losses are observed in the TGA curves: 100–200°C, 200–300°C, and 300–550°C. The DTA curve shows an endothermic peak below 200°C accompanied by small weight loss of about 5%, which corresponds to the removal of excess water and ethylene glycol. The next peak is observed between 200 and 300°C, and it is related to the decomposition of the residual citric acid. This results in a weight loss of ~55%. The last event is represented by the strong exothermic peak located between 300 and 550°C with a weight loss of 35%, which is attributed to the decomposition of the organic resin formed in the Pechini process. After 550°C, the residual weight remains constant.

The XRD patterns of the nanoparticles obtained after calcination at 400°C (a) and 600°C (b) at different times are shown in Figure 2. The sample annealed at 400°C for 15 min shows diffraction peaks corresponding to the hcp and fcc phases for Ni. The specific diffraction peaks (010), (002), (011), (012), (110), (103), (112), and (201) correspond to the hcp structure, whereas the (111), (200), and (220) to the fcc structure. These diffraction peaks are in agreement with JCPDS nos. 45-1027 and 04-0850, respectively [10, 11]. The sample annealed for 1 h shows the same peaks as those mentioned before. The small peak located at 43.3° is associated with NiO. Upon increasing the calcination time to
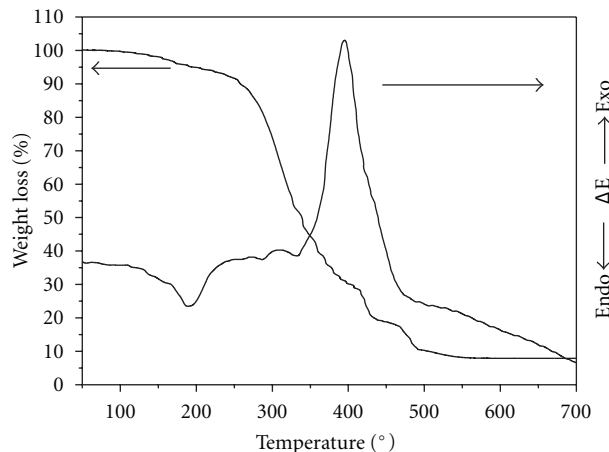

Figure 1: TGA-DTA analyses of the precursor material.

2 h, the nanoparticles are composed by Ni/NiO phase. The diffraction peaks at 37.25, 43.30, 62.92, 75.45, and 79.35° correspond to the (111), (200), (220), (311), and (222) planes of the fcc phase NiO and are in excellent agreement with JCPDS no. 04-0835 [12]. It is important to note that only the fcc phase for Ni is present.

During the calcination process precursor material decomposition occurs. This decomposition produces a CO/CO$_2$-rich atmosphere. Such atmosphere promotes the reduction of the metallic salt, resulting in Ni nanoparticles. This atmosphere can prevent Ni oxidation for calcination times shorter than 1 h. For calcination treatments longer than 1 h, Ni nanoparticles start to oxidize and form Ni/NiO nanoparticles. When the temperature is increased up to 600°C, only the sample annealed for 15 minutes shows this Ni/NiO structure. Clearly, the samples annealed for more than 1 h show only NiO phase (Figure 2(b)).

It is important to mention that the formation of hcp Ni structure was not expected. According to the literature this is a metastable phase and only can be obtained under specific conditions. Here, two main processes for the formation of the hcp phase have been suggested, (a) as a result of a fast thermal decomposition of the precursor materials [13] and (b) the protection of the Ni nanoparticles with graphite [14]. Both processes mentioned could take place in the citric assisted Pechini-type method. A strong exothermic reaction causes the increase of the temperature favoring a fast decomposition of the precursors and the subsequent graphite formation as reported for different systems [15, 16].

For the samples prepared at 400°C, the phase percentages obtained by the whole-profile fitting program are shown in Table 1. Following this preparation method, different Ni phase percentages can be easily controlled by the calcination time. As can be seen in Table 1, while the hcp Ni phase percentage decreases with increasing of the calcination time, the fcc Ni phase increases. It means that during the calcination the hcp phase is transformed to fcc phase and the number of fcc Ni nanoparticles is increased. A long calcination time is needed in order to obtain Ni/NiO nanoparticles.
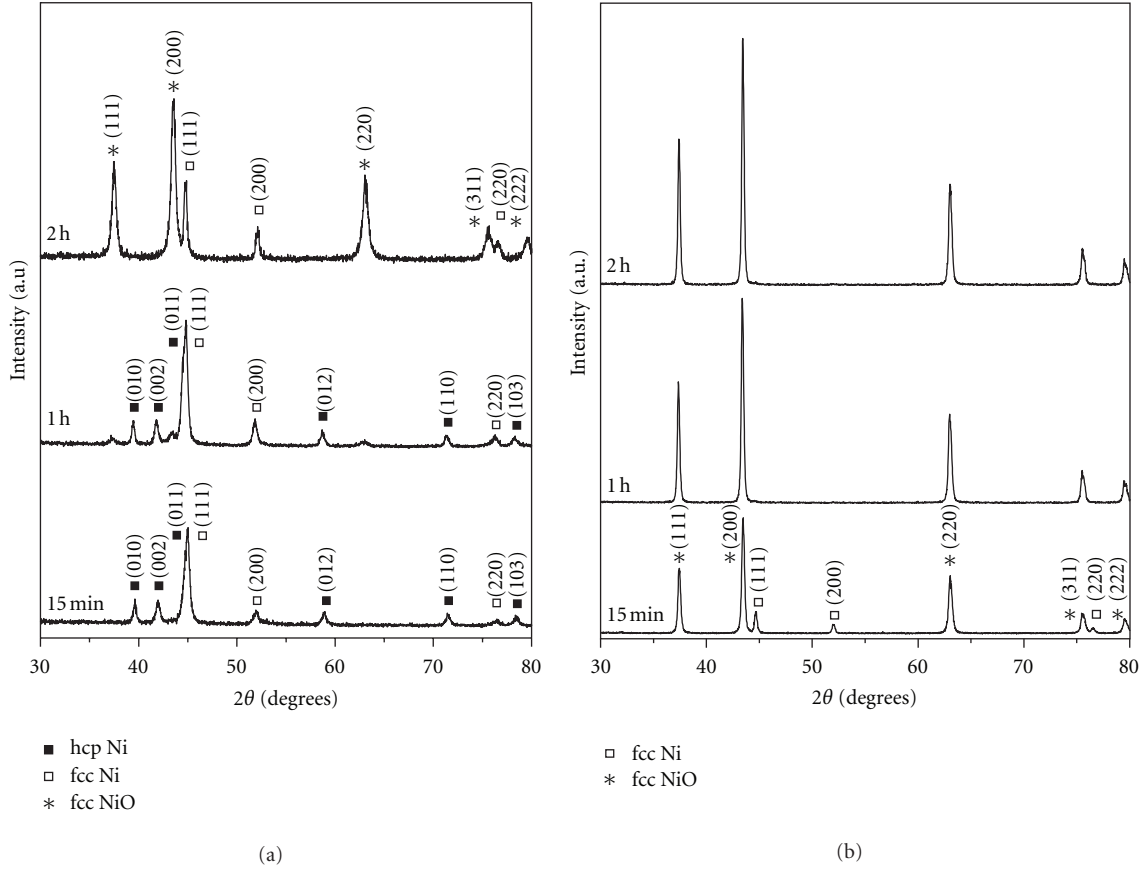
Figure 2: XRD patterns of nanoparticles obtained at 400°C (a) and 600°C (b) for 15 min, 1 h, and 2 h.

Table 1: Particle size, phase percentage, saturation magnetization, and coercivity of the samples obtained at 400°C for 15 min, 1 h, and 2 h.

Time	Particle size (nm)			Phase percentage (%)			Ms (emu/g)	Hc (Oe)
	hcp Ni	fcc Ni	fcc NiO	hcp Ni	fcc Ni	fcc NiO		
15 min	17.0	9.8	—	65.47	34.53	—	2.8	86
1 h	22.0	30.0	—	53.53	43.46	3.01	3.9	60
2 h	—	30.2	18.4	—	48.74	51.26	5.2	150

The sizes of Ni and Ni/NiO nanoparticles were calculated from the X-ray peak broadening of the most intense reflection using the Scherrer's formula [17], which is represented as

$$d = \frac{k\lambda}{\beta \cos\theta}, \qquad (1)$$

where k is the shape coefficient for reciprocal lattice point (here, assuming $k = 0.95$), λ the wavelength of the X-ray radiation (1.54056 Å), β is the full width at half maximum (FWHM) of the peak, and θ is the Bragg angle.

The particle sizes of the samples obtained at 400°C at 15 min, 1 h, and 2 h calculated by (1) are showed in Table 1. As expected, particle sizes monotonically increase with the increasing calcination time. The particle size of the samples is in the range of 17–22 nm for hcp Ni, 9.8–30.2 nm for fcc Ni, and 18 nm for fcc NiO.

The magnetic properties of the samples obtained at 400°C for 15 min, 1 h, and 2 h were studied by recording the hysteresis (M-H) loops, as shown in Figure 3. The values of the coercive field and saturation magnetization of the samples are given in Table 1. The sample obtained at 15 min shows a ferromagnetic behavior with a saturation magnetization (Ms) of 2.8 emu/g. After 1 h of calcination, the Ms increases to 3.9 emu/g and to 5.2 emu/g for the sample annealed for 2 h. This increase in the saturation magnetization could be related to the increase of the fcc-Ni phase (ferromagnetic phase) with the calcination time. As previously mentioned, according to the XRD patterns after heat treatments of 15 min and 1 h, the samples consist in a mixture of hcp-Ni and fcc-Ni phases. As the calcination time increased, the hcp Ni was transformed to fcc Ni. According to the literature, the magnetic behavior of the hcp-Ni is not clear. Theoretically, the hcp Ni can be ferromagnetic [18], and some experimental proofs showed this behavior [19, 20].
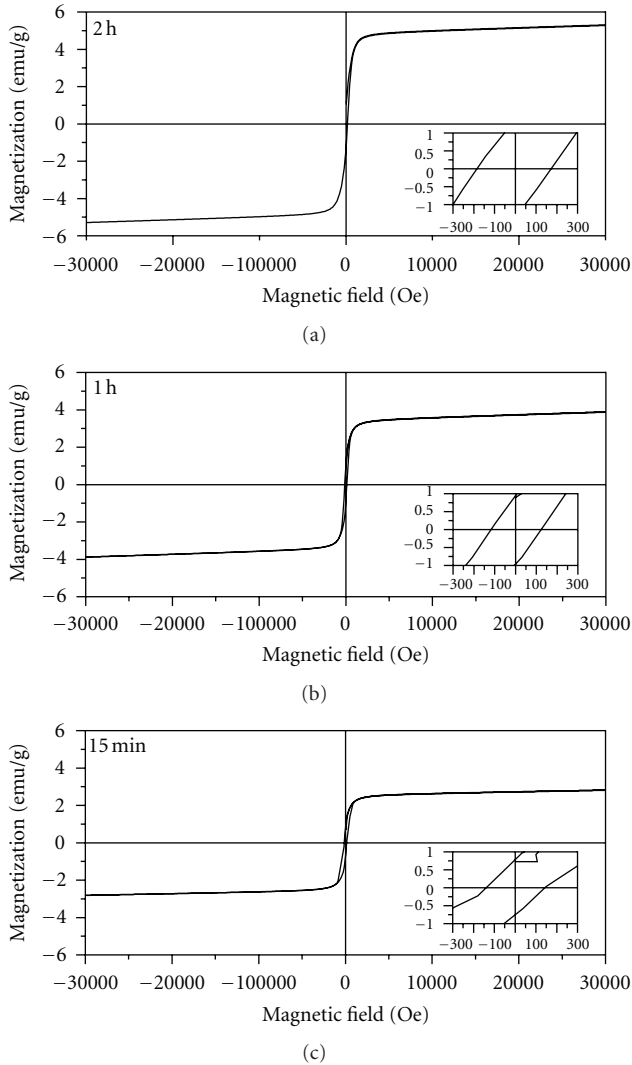
(a)

(b)

(c)

Figure 3: Hysteresis curves of the samples obtained at 400°C for 15 min, 1 h, and 2 h.

(a)

(b)

Figure 4: Low-magnification TEM image of the Ni/NiO nanoparticles obtained at 400°C for 2 h. (b) HRTEM image of the Ni/NiO nanoparticles.

However, other studies mentioned that the hcp Ni can also be nonmagnetic or antiferromagnetic. In our work, when the system is composed by hcp Ni and fcc Ni (sample obtained at 15 min), the saturation magnetization value is lower than the samples obtained at 1 h and 2 h. As the amount of fcc Ni is increased, a higher saturation magnetization value is obtained, supporting the nonmagnetic or weak magnetic behavior of the hcp phase. Similar results have been reported in the literature [21, 22].

The prepared nickel nanoparticles are dispersed in carbon and/or NiO, so it is considered as a solid solution of nickel atoms in carbon and/or NiO; therefore the specific magnetization is low. Additionally, the magnetization could be further reduced due to the existence of random Ni magnetic moments at the nanoparticles surface and/or nonmagnetic Ni (or NiO) atoms located at the interfaces between the Ni nanoparticles and the amorphous carbon matrix or the NiO phase [23, 24].
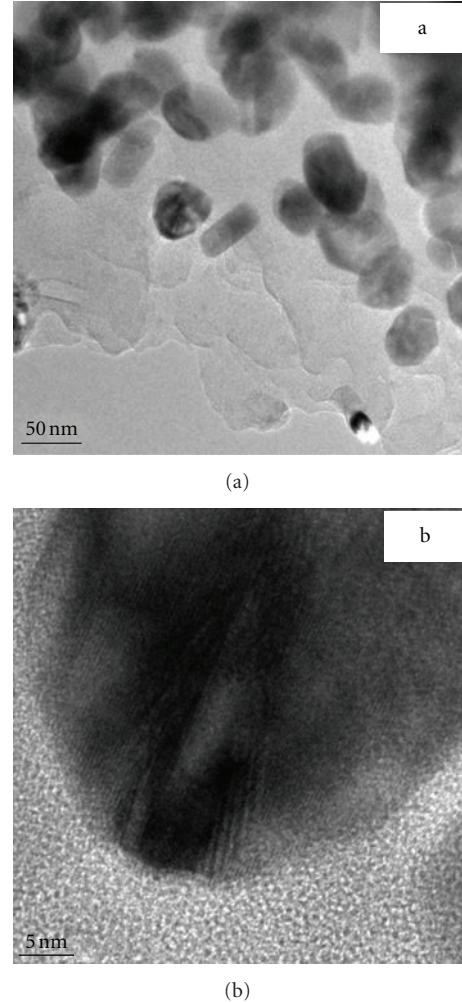
Also from Figure 3, we can observe that the coercive field is not zero for all the samples. The coercivity for the 15 min sample was 86 Oe. The samples obtained at 1 h and 2 h showed coercivities of 60 Oe and 150 Oe, respectively. The increase in the coercive value of the 2 h sample could be related to a better isolation of the ferromagnetic phase in the antiferromagnetic/nonmagnetic matrix. Loop shifts were not observed, indicating the absence of exchange bias effects (inserts Figure 3).

TEM image of the Ni and Ni/NiO nanoparticles obtained at 400°C for 2 h is shown in Figure 4(a). According to the image, the sample is composed by crystalline particles embedded in carbon amorphous matrix. The shape of the nanoparticles varies from nearly spherical to ellipsoidal and irregular morphologies. The average particle size varies from 10 to 30 nm, in agreement with the XRD results. Figure 4(b) shows the observed structure for the Ni/NiO nanoparticles. From the images, the exact morphology of the Ni/NiO nanoparticles is hard to estimate. Highly disordered regions are visible, where a long-range crystalline order is not clearly

observable (Figure 4(b)). Here, it is possible to guess that the relatively long calcination time favors the formation of NiO on top of the Ni particles, acting as a passivating region and preventing the further growing of Ni nanoparticles, and thus isolating them. The formation of this passivating region has been reported in related works [26]. This mechanism promotes a close contact between the Ni and NiO in the nanoparticles [27], but also could lead to a disordered growth of the NiO matrix.

4. Conclusions

In summary, we prepared hcp and fcc Ni and Ni/NiO nanoparticles by simply changing the processing conditions, specifically, the time and temperature of calcination of the precursor material. Ni nanoparticles showed a mixture of fcc and hcp phases. When the time and temperature of calcination increased, a phase transformation from hcp Ni to fcc Ni and the formation of Ni/NiO were observed. The magnetic properties of the samples, ferromagnetic in nature, reflected the proposed phase transition. Based on the versatility of the method, it can be extended to prepare other metal nanoparticles and its respective metal/metal oxide nanoparticles, such as those of Fe, Cu, and Co.
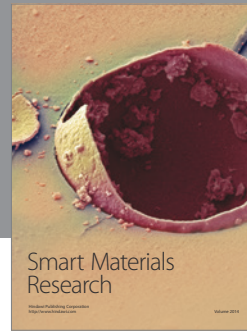
Acknowledgments

References

[1] M. P. Pileni, "Magnetic fluids: fabrication, magnetic properties, and organization of nanocrystals," *Advanced Funtional Materials*, vol. 11, no. 5, pp. 323–336, 2001.

[2] J. Park, E. Kang, S. U. Son et al., "Monodisperse nanoparticles of Ni and NiO: synthesis, characterization, self-assembled superlattices, and catalytic applications in the suzuki coupling reaction," *Advanced Materials*, vol. 17, no. 4, pp. 429–434, 2005.

[3] J. Sort, J. Nogués, X. Amils, S. Suriñach, J. S. Muñoz, and M. D. Baró, "Room temperature magnetic hardening in mechanically milled ferromagnetic-antiferromagnetic composites," *Journal of Magnetism and Magnetic Materials*, vol. 219, no. 1, pp. 53–57, 2000.

[4] I. Hotovy, J. Huran, P. Siciliano, S. Capone, L. Spiess, and V. Rehacek, "The influences of preparation parameters on NiO thin film properties for gas-sensing application," *Sensors and Actuators, B*, vol. 78, no. 1–3, pp. 126–132, 2001.

[5] I. S. Lee, N. Lee, J. Park et al., "Ni/NiO core/shell nanoparticles for selective binding and magnetic separation of histidine-tagged proteins," *Journal of the American Chemical Society*, vol. 128, no. 33, pp. 10658–10659, 2006.

[6] Y. Mi, D. Yuan, Y. Liu, J. Zhang, and Y. Xiao, "Synthesis of hexagonal close-packed nanocrystalline nickel by a thermal reduction process," *Materials Chemistry and Physics*, vol. 89, no. 2-3, pp. 359–361, 2005.

[7] Y. Hou, H. Kondoh, T. Ohta, and S. Gao, "Size-controlled synthesis of nickel nanoparticles," *Applied Surface Science*, vol. 241, no. 1-2, pp. 218–222, 2005.

[8] Y. Z. Zhou, J. S. Chen, B. K. Tay et al., "Ni-NiO core-shell nanoclusters with cubic shape by nanocluster beam deposition," *Applied Physics Letters*, vol. 90, no. 4, Article ID 043111, 2007.

[9] M. P. Pechini, " Method of preparing lead and alkaline earth titanates and niobates and coating method using the same to form a capacitor," US patent number 3330697, 1967.

[10] Joint Committee on Powder Diffraction Standards (JCPDS) card no. 45–1027.

[11] Joint Committee on Powder Diffraction Standards (JCPDS) card no. 04-0850.

[12] Joint Committee on Powder Diffraction Standards (JCPDS) card no. 04-0835.

[13] Y. T. Jeon, J. Y. Moon, G. H. Lee, J. Park, and Y. Chang, "Comparison of the magnetic properties of metastable hexagonal close-packed Ni nanoparticles with those of the stable face-centered cubic Ni nanoparticles," *Journal of Physical Chemistry B*, vol. 110, no. 3, pp. 1187–1191, 2006.

[14] V. Rodríguez-González, E. Marceau, P. Beaunier, M. Che, and C. Train, "Stabilization of hexagonal close-packed metallic nickel for alumina-supported systems prepared from Ni(II) glycinate," *Journal of Solid State Chemistry*, vol. 180, no. 1, pp. 22–30, 2007.

[15] H. Lee, M. Hong, S. Bae, H. Lee, E. Park, and K. Kim, "A novel approach to preparing nano-size Co_3O_4-coated Ni powder by the Pechini method for MCFC cathodes," *Journal of Materials Chemistry*, vol. 13, no. 10, pp. 2626–2632, 2003.

[16] M. Kakihana, "'Sol-Gel' preparation of high temperature superconducting oxides," *Journal of Sol-Gel Science and Technology*, vol. 6, no. 1, pp. 7–55, 1996.

[17] B. D. Cullity, *Elements of X-Ray Diffraction*, Addison-Wesley, New York, USA, 1978.

[18] X. He, L. T. Kong, and B. X. Liu, "Calculation of ferromagnetic states in metastable bcc and hcp Ni by projector-augmented wave method," *Journal of Applied Physics*, vol. 97, no. 10, Article ID 106107, 2005.

[19] X. Luo, Y. Chen, G. H. Yue, D. L. Peng, and X. Luo, "Preparation of hexagonal close-packed nickel nanoparticles via a thermal decomposition approach using nickel acetate tetrahydrate as a precursor," *Journal of Alloys and Compounds*, vol. 476, no. 1-2, pp. 864–868, 2009.

[20] V. Tzitzios, G. Basina, M. Gjoka et al., "Chemical synthesis and characterization of hcp Ni nanoparticles," *Nanotechnology*, vol. 17, no. 15, pp. 3750–3755, 2006.

[21] C. N. Chinnasamy, B. Jeyadevan, K. Shinoda, K. Tohji, A. Narayanasamy, and S. Hisano, "Synthesis and magnetic properties of face-centered-cubic and hexagonal-close-packed Ni nanoparticles through polyol process," *Journal of Applied Physics*, vol. 97, no. 10, Article ID 10J309, pp. 1–3, 2005.

[22] M. Han, Q. Liu, J. He, Y. Song, Z. Xu, and J. Zhu, "Controllable synthesis and magnetic properties of cubic and hexagonal phase nickel nanocrystals," *Advanced Materials*, vol. 19, no. 8, pp. 1096–1100, 2007.

[23] D. W. Wang, F. Li, G. Q. Lu, and H. M. Cheng, "Synthesis and dye separation performance of ferromagnetic hierarchical porous carbon," *Carbon*, vol. 46, no. 12, pp. 1593–1599, 2008.

[24] L. Del Bianco, F. Boscherini, A. L. Fiorini et al., "Exchange bias and structural disorder in the nanogranular Ni/NiO system

produced by ball milling and hydrogen reduction," *Physical Review, B*, vol. 77, no. 9, Article ID 094408, 2008.

[25] J. Nogués, J. Sort, V. Langlais et al., "Exchange bias in nanostructures," *Physics Reports*, vol. 422, no. 3, pp. 65–117, 2005.

[26] Y. Li, M. Cai, J. Rogers, Y. Xu, and W. Shen, "Glycerol-mediated synthesis of Ni and Ni/NiO core-shell nanoparticles," *Materials Letters*, vol. 60, no. 6, pp. 750–753, 2006.

[27] A. Roy, V. Srinivas, S. Ram, J. A. De Toro, and U. Mizutani, "Structure and magnetic properties of oxygen-stabilized tetragonal Ni nanoparticles prepared by borohydride reduction method," *Physical Review, B*, vol. 71, no. 18, pp. 184443–184410, 2005.

Journal of
Nanotechnology

International Journal of
Corrosion

International Journal of
Polymer Science

Smart Materials
Research

Journal of
Composites

BioMed
Research International

Journal of
Materials

Journal of
Metallurgy

Hindawi

Submit your manuscripts at
http://www.hindawi.com

Journal of
Nanoparticles

Advances in
Materials Science and Engineering

Scientifica

Journal of
Nanomaterials

The Scientific
World Journal

International Journal of
Biomaterials

Journal of
Nanoscience

Journal of
Coatings

Journal of
Crystallography

Journal of
Ceramics

Journal of
Textiles